Computation and semiclassical analysis of scaled spectra for excitons with two-dimensional Coulomb interaction in a quantum well

Bachelor's Thesis by
David Mayer

20.09.2025

Examiner: Prof. Dr. Jörg Main

submitted to

Universität Stuttgart

Institute for Theoretical Physics I
Pfaffenwaldring 57, 70569 Stuttgart

Contents

1 Introduction

The absorption of a photon inside an insulating crystal can create a bound electron-hole pair. The electron and hole interact via the Coulomb potential similar to the binding of the electron to the proton in a hydrogen atom, forming a bound state known as an exciton. This process is crucial in understanding the optical properties of semiconductors and insulators, as excitons play a significant role in light absorption and emission processes. Excitons are quasiparticles moving through the crystal, transporting energy without transporting charge.

Studying the behavior of excitons is fundamental for interpreting the optical and electronic properties of materials in semiconductor physics. The properties of finite-sized crystals differ from those of the bulk materials, where the confinement of the exciton can be described by quantum wells [1]. In these wells, the motion of the exciton is confined in one dimension, leading to quantized energy levels.

In this thesis, we investigate the scaled energy spectra of excitons in cuprous oxide which is a non-integrable problem. We consider the integrable system by reducing the Coulomb interaction to a two-dimensional problem. By combining semiclassical methods, classical dynamics, quantization conditions, and numerical computations we investigate how the periodic trajectories contribute to the energy spectra.

For simplicity, we consider an uncoupled system in which the Coulomb potential depends solely on the in-plane separation between electron and hole. We compute the classical action along each periodic trajectory and compare those results to predictions from the semiclassical approach by applying a Fourier transform to the density of states.

In order to determine the trajectories we solve the equations of motion for the periodic orbits of the exciton in the two-dimensional Coulomb potential. Furthermore, we investigate different triplets of the winding numbers characterizing each trajectory. The aim of this thesis is to compute and analyze the scaled spectra of excitons confined in a quantum well using semiclassical and classical methods, and to connect periodic orbits to spectral features.

2 Theoretical Foundation

2.1 Hamiltonian for Excitons in a Quantum Well

An exciton can be described as a bound state of an electron and a hole with a Coulomb interaction between them. The Hamiltonian for excitons in a cuprous oxide quantum well can be written as

$$H = \frac{\mathbf{p}_\mathrm{e}^2}{2m_\mathrm{e}} + \frac{\mathbf{p}_\mathrm{h}^2}{2m_\mathrm{h}} - \frac{e^2}{4\pi\varepsilon_0\varepsilon_\mathrm{r}} \frac{1}{|\mathbf{r}_\mathrm{e} - \mathbf{r}_\mathrm{h}|} + V_\mathrm{QW}(z_\mathrm{e}) + V_\mathrm{QW}(z_\mathrm{h}), \tag{2.1}$$

where $\mathbf{p}_\mathrm{e}$ and $\mathbf{p}_\mathrm{h}$ are the momenta of the electron and hole, $m_\mathrm{e} = 0.99\,m_0$ and $m_\mathrm{h} = 0.69\,m_0$ are their respective masses, e is the elementary charge, ε_0 the vacuum permittivity, $\varepsilon_\mathrm{r} = 7.5$ is the dielectric constant, and $\mathbf{r}_\mathrm{e,h}$ is the position vector of the electron and hole. The term $V_\mathrm{QW}(z_\mathrm{e,h})$ (cf. equation (2.16)) represents the quantum-well potential along the z-axis, which confines the exciton inside the medium. Subsequently, z_e and z_h are the respective positions inside the quantum well.

Finally, we introduce cylindrical coordinates for the relative motion of the electron and hole [2]. Thus, we also neglect center-of-mass (COM) motion in the (x, y) plane. The cylindrical coordinates simplify the calculations because we can later on reduce the Coulomb term to the two-dimensional interaction. Otherwise, the problem would only be solvable by numerically intensive calculations. The Hamiltonian in cylindrical coordinates becomes

$$\begin{aligned} H = &-\frac{\hbar^2}{2\mu}\left(\frac{\partial^2}{\partial\rho^2} + \frac{m^2 - 1/4}{\rho^2}\right) - \frac{\hbar^2}{2m_\mathrm{e}}\frac{\partial^2}{\partial z_\mathrm{e}^2} - \frac{\hbar^2}{2m_\mathrm{h}}\frac{\partial^2}{\partial z_\mathrm{h}^2} \\ &- \frac{e^2}{4\pi\varepsilon_0\varepsilon_\mathrm{r}} \frac{1}{\sqrt{\rho^2 + (z_\mathrm{e} - z_\mathrm{h})^2}} + V_\mathrm{QW}(z_\mathrm{e}) + V_\mathrm{QW}(z_\mathrm{h}) \end{aligned} \tag{2.2}$$

where ρ is the in-plane distance between electron and hole with coordinates $x_\mathrm{e,h}, y_\mathrm{e,h}$,

$$\rho = \sqrt{(x_\mathrm{e} - x_\mathrm{h})^2 + (y_\mathrm{e} - y_\mathrm{h})^2}, \tag{2.3}$$

and μ is the reduced mass, defined as

$$\mu = \frac{m_\mathrm{e} m_\mathrm{h}}{m_\mathrm{e} + m_\mathrm{h}}. \tag{2.4}$$

The separation of the Schrödinger equation yields a separation constant m, which is a good quantum number. It is an integer quantum number; however, we set $m = 1/2$ in order to completely eliminate the centrifugal term.

2.1.1 Scaling of the system and scaled Schrödinger equation

The general representation of the Hamiltonian for wave functions of the form $\chi(\rho, z_\mathrm{e}, z_\mathrm{h}) = \sqrt{\rho}\Psi(\rho, z_\mathrm{e}, z_\mathrm{h})$ is given by

$$\begin{aligned} H = {} & \frac{p_{z_\mathrm{e}}^2}{2m_\mathrm{e}} + \frac{p_{z_\mathrm{h}}^2}{2m_\mathrm{h}} + \frac{p_\rho^2}{2\mu} + \frac{(m^2 - 1/4)\hbar^2}{2\mu\rho^2} \\ & - \frac{1}{\sqrt{\rho^2 + (z_\mathrm{e} - z_\mathrm{h})^2}} + V_\mathrm{QW}(z_\mathrm{e}) + V_\mathrm{QW}(z_\mathrm{h}). \end{aligned} \tag{2.5}$$

The centrifugal term can be neglected in the classical limit and for small quantum numbers. We set $m = 1/2$ in order to completely eliminate the centrifugal term. We introduce the boundary condition

$$\chi(\rho) = c\rho + \mathcal{O}(\rho^2) \tag{2.6}$$

for small ρ. Furthermore, we can now treat ρ as a Cartesian coordinate. The dynamics and eigenstates of the system depend on the quantum well width L and the energy E. In the following we introduce the scaled momenta

$$p_{z_{\mathrm{e,h},\rho}} = \frac{1}{\sqrt{L}} \tilde{p}_{z_{\mathrm{e,h},\rho}} \tag{2.7}$$

and scaled coordinates

$$z_\mathrm{e,h} = L\tilde{z}_\mathrm{e,h}, \quad \rho = L\tilde{\rho}. \tag{2.8}$$

Here the scaled coordinates are defined in the interval $\tilde{z} \in [-1/2, 1/2]$. This leads to the scaled Hamiltonian

$$\begin{aligned} LH = LE = \tilde{E} = {} & \frac{\tilde{p}_{z_\mathrm{e}}^2}{2m_\mathrm{e}} + \frac{\tilde{p}_{z_\mathrm{h}}^2}{2m_\mathrm{h}} + \frac{\tilde{p}_\rho^2}{2\mu} \\ & - \frac{1}{\sqrt{\tilde{\rho}^2 + (\tilde{z}_\mathrm{e} - \tilde{z}_\mathrm{h})^2}} + \tilde{V}_\mathrm{e} + \tilde{V}_\mathrm{h}. \end{aligned} \tag{2.9}$$

Now the classical dynamics of the system only depends on one parameter, the scaled energy $\tilde{E} = LE$. The commutator relation

$$[\tilde{\rho}, \tilde{p}_\rho] = \frac{1}{\sqrt{L}} [\rho, p_\rho] . \tag{2.10}$$

yields an effective Planck's constant $\hbar_{\text{eff}} = \hbar/\sqrt{L}$, which goes to zero in the classical limit $L \to \infty$. The scaled Schrödinger equation can be written as

$$\left[-\frac{1}{2m_\text{e}} \frac{d^2}{d\tilde{z}_\text{e}^2} - \frac{1}{2m_\text{h}} \frac{d^2}{d\tilde{z}_\text{h}^2} - \frac{1}{2\mu} \frac{d^2}{d\tilde{\rho}^2} \right] \hbar_{\text{eff}}^2 \chi = \left[\tilde{E} + \frac{1}{\sqrt{\tilde{\rho}^2 + (\tilde{z}_\text{e} - \tilde{z}_\text{h})^2}} \right] \chi \tag{2.11}$$

with corresponding eigenvalues $\lambda = \frac{\hbar^2}{L} = \hbar_{\text{eff}}^2$.

2.1.2 Two-dimensional Coulomb interaction

In order to simplify the problem and the intensity of numerical calculations, we reduce the Coulomb potential by neglecting the z-dependence, assuming a two-dimensional Coulomb interaction. Furthermore, the centrifugal term drops because we set $m = 1/2$. In this simplification, the electron–hole separation reduces to

$$|\mathbf{r}_\text{e} - \mathbf{r}_\text{h}| = \sqrt{\rho^2 + \left(z_\text{e} - z_\text{h}\right)^2} \to \rho. \tag{2.12}$$

The Hamiltonian in those coordinates simplifies to

$$H = \frac{p_\rho^2}{2\mu} + \frac{p_{z,\text{e}}^2}{2m_\text{e}} + \frac{p_{z,\text{h}}^2}{2m_\text{h}} - \frac{e^2}{4\pi\varepsilon_0\varepsilon_\text{r}} \frac{1}{\rho} + V_{\text{QW}}(z_\text{e}) + V_{\text{QW}}(z_\text{h}). \tag{2.13}$$

We reduced the Coulomb interaction to a two-dimensional form, depending only on the in-plane distance between the electron and the hole ρ. The choice $m = 1/2$ shifts the Rydberg energy from

$$E = -\frac{\mu e^4}{32\pi^2 \varepsilon_0^2 \hbar^2 (n - 1/2)^2} \tag{2.14}$$

to

$$E = -\frac{\mu e^4}{32\pi^2 \varepsilon_0^2 \hbar^2 n^2}. \tag{2.15}$$

where n is the principal quantum number for the in-plane bound states of the hydrogen atom.

2.2 Potential Well

The confinement of the exciton inside cuprous oxide in the z-direction can be modeled by an infinite potential well. For the electron and hole coordinates $z_{\mathrm{e,h}}$ the potential $V_{\mathrm{QW}}(z_{\mathrm{e,h}})$ is defined as

$$V_{\mathrm{QW}}(z_{\mathrm{e,h}}) = \begin{cases} 0 & \text{for } |z_{\mathrm{e,h}}| < L/2, \\ \infty & \text{for } |z_{\mathrm{e,h}}| \geq L/2, \end{cases} \tag{2.16}$$

where L is the width of the quantum well. In the following, we introduce exciton Hartree units for the energy. We set

$$e = \hbar = \mu = (4\pi\varepsilon_0\varepsilon_{\mathrm{r}})^{-1} = 1 \tag{2.17}$$

and measure lengths L in units of the exciton Bohr radius

$$a_0 = \frac{4\pi\varepsilon_0\varepsilon_{\mathrm{r}}\hbar^2}{\mu e^2}. \tag{2.18}$$

In the following, the masses $m_{\mathrm{e,h}}$ are expressed relative to μ, i.e.,

$$m_{\mathrm{e}} \to \frac{m_{\mathrm{e}}}{\mu}, \quad m_{\mathrm{h}} \to \frac{m_{\mathrm{h}}}{\mu}. \tag{2.19}$$

2.2.1 Potential well solutions

We simplify the problem by separating it into an infinite potential well in the z-direction and a two-dimensional Coulomb problem in the xy-plane. The time-independent Schrödinger equation for the quantum well in the z-direction can be written as

$$\hat{H}\,\Psi_{\mathrm{e,h}}(z_{\mathrm{e,h}}) = \left(-\frac{\hbar^2}{2m_{\mathrm{e,h}}}\frac{\partial^2}{\partial z^2} + V_{\mathrm{QW}}(z_{\mathrm{e,h}})\right)\Psi_{\mathrm{e,h}}(z_{\mathrm{e,h}}) = E\,\Psi_{\mathrm{e,h}}(z_{\mathrm{e,h}}). \tag{2.20}$$

The boundary conditions for the potential well are given by equation (2.16), i.e.,

$$\Psi_{\mathrm{e,h}}(z_{\mathrm{e,h}}) = 0 \quad \text{for} \quad |z_{\mathrm{e,h}}| = \tfrac{L}{2}. \tag{2.21}$$

Inside the quantum well, we set the potential $V_{\mathrm{QW}}(z_{\mathrm{e,h}})$ to zero (cf. equation (2.21)), which leads to the usual standing-wave solutions for the eigenfunctions of the electron and hole,

$$\Psi_{z_{\mathrm{e,h}}}(z_{\mathrm{e,h}}) = \sqrt{\frac{2}{L}}\,\sin\left(\frac{N_{\mathrm{e,h}}\pi z_{\mathrm{e,h}}}{L}\right), \tag{2.22}$$

with corresponding eigenenergies

$$E_{N_{\mathrm{e,h}}} = \frac{N_{\mathrm{e,h}}^2 \pi^2 \hbar^2}{2\, m_{\mathrm{e,h}}\, L^2}, \tag{2.23}$$

where the quantum numbers are $N_{\mathrm{e,h}} \in \mathbb{N}$. In exciton Hartree units (cf. Eqs. (2.17), (2.18)), the energies of the electron and hole in the quantum well can be expressed as

$$E_{N_{\mathrm{e,h}}} = \frac{N_{\mathrm{e,h}}^2 \pi^2 \mu^2}{2 m_{\mathrm{e,h}} (L/a_0)^2}. \tag{2.24}$$

The energy of the exciton inside the quantum well is then given by the sum of the energies of the electron and hole in the quantum well (cf. equation (2.24)) and the two-dimensional Coulomb interaction (cf. equation (2.15)). In exciton Hartree units, the total energy of the exciton can be written as

$$E_{N_{\mathrm{e}},N_{\mathrm{h}},n} = \frac{\pi^2 \mu}{2(L/a_0)^2} \left(\frac{N_{\mathrm{e}}^2}{m_{\mathrm{e}}} + \frac{N_{\mathrm{h}}^2}{m_{\mathrm{h}}} \right) - \frac{1}{2n^2}. \tag{2.25}$$

2.3 Semiclassical Framework

In semiclassical physics, quantum states are compared with their classical counterparts while combining classical mechanics with quantum principles. The Bohr–Sommerfeld quantization condition states that the action of systems with one degree of freedom, i.e. $f = 1$, is given by

$$S(E) = \oint p\, dq \tag{2.26}$$

for closed trajectories $q(t)$ in phase space and takes discrete values

$$S(E) = 2\pi\hbar n, \qquad n \in \mathbb{N}. \tag{2.27}$$

Originally developed from heuristic and empirical considerations in the early 20th century, it provides a simple but effective framework for linking classical and quantum mechanics. In modern terms, it emerges naturally from the WKB approximation as a quantization of the action variable in integrable systems.

2.3.1 Action–angle variables

For integrable Hamiltonian systems with f degrees of freedom, it is convenient to find coordinates in which the Hamiltonian does not depend on the spatial coordinates Q, i.e.,

$$H' = H'(P) \tag{2.28}$$

where P are the momenta conjugate to the coordinates Q. For this matter we can use canonical transformations. The equations of motion in these coordinates are given by

$$\dot{P}_i = -\frac{\partial H'}{\partial Q_i} = 0, \quad \dot{Q}_i = \frac{\partial H'}{\partial P_i}, \qquad i = 1, \ldots, f. \tag{2.29}$$

In this case, the Hamiltonian is constant along trajectories in phase space and therefore the momenta P_i stay constant in motion. The derivative of the trajectories $\dot{Q}_i$ can be integrated to

$$Q_i(t) = Q_i(0) + t\frac{\partial H'}{\partial P_i}. \tag{2.30}$$

For a closed system this resembles the motion on an f-dimensional torus. The necessary transformations

$$(q_i, p_i) \to (Q_i, P_i) \tag{2.31}$$

for finding the cyclic variables are given by the generating function $F_2 = S(q, P, t)$ where

$$p_i = \frac{\partial S}{\partial q_i}, \quad Q_i = \frac{\partial S}{\partial P_i}. \tag{2.32}$$

The generating function is defined by the Hamilton-Jacobi equation

$$H\left(\frac{\partial S}{\partial q_i}, Q_i, t\right) + \frac{\partial S}{\partial t} = 0. \tag{2.33}$$

If such a solution S exists, the Hamilton function is called integrable. For each integrable system a separable subclass exists, where the Hamilton–Jacobi equation splits into f ordinary differential equations. By using the separation ansatz

$$S = \sum_{i=1}^{f} S_i(q_i, \alpha_i, \ldots, \alpha_f) \tag{2.34}$$

with separation constants α_i, the Hamilton–Jacobi equation separates into f ordinary differential equations

$$H_i\left(\frac{\partial S_i}{\partial q_i}, q_i\right) = \alpha_i. \tag{2.35}$$

We define the action variables $J_i(\alpha_i)$ so that

$$\frac{\partial H}{\partial J_i} = \omega_i \tag{2.36}$$

where ω_i is the frequency of the motion on the torus. The generating function is then given by

$$\tilde{S}(\boldsymbol{q}, \boldsymbol{J}) = S(\boldsymbol{q}, \boldsymbol{\alpha}(\boldsymbol{J})), \quad H(\boldsymbol{\alpha}) \to \tilde{H}(\boldsymbol{J}). \tag{2.37}$$

The action variables are given by the integrals

$$J_i = \frac{1}{2\pi} \oint p_i \, dq_i = \frac{1}{2\pi} \oint \frac{\partial S_i(q_i, \boldsymbol{\alpha})}{\partial q_i} \, dq_i. \tag{2.38}$$

The conjugate angle variables ϑ_i are given by

$$\vartheta_i = \frac{\partial \tilde{S}(q_i, J_i)}{\partial J_i}. \tag{2.39}$$

2.3.2 Wentzel–Kramers–Brillouin–Jeffreys approximation

The WKB method is a semiclassical approximation for systems with one degree of freedom. It is particularly useful for systems where the potential varies slowly compared to the wavelength of the particle. The WKB approximation helps to solve the Schrödinger equation and leads to quantization conditions that relate the classical action to quantum states. We start with the time-independent Schrödinger equation in one dimension,

$$\left[-\frac{\hbar^2}{2m} \frac{d^2 \Psi}{dq^2} + V(q) \right] \Psi = E \Psi. \tag{2.40}$$

By inserting the ansatz

$$\Psi(q) = A(q) \exp\left(\frac{i}{\hbar} S(q) \right) = \exp\left(i \frac{\omega(q)}{\hbar} \right) \tag{2.41}$$

where the coefficient $\omega(q)$ is defined as

$$\omega(q) = S(q) + \frac{\hbar}{i} \ln\left[A(q) \right] \tag{2.42}$$

into the Schrödinger equation and neglecting terms of order $\hbar^2$ we obtain

$$A = c(S)^{-\frac{1}{2}} \tag{2.43}$$

and

$$S'^2 = 2m(E - V) + \hbar^2 \left[\frac{3}{4} \left(\frac{S''}{S'} \right)^2 - \frac{1}{2} \frac{S'''}{S'} \right]. \tag{2.44}$$

After expanding with respect to $\hbar$ and dropping higher-order terms, we obtain the Hamilton–Jacobi equation

$$S_0^2 = 2m(E - V). \tag{2.45}$$

Solving for S_0 gives the WKB quantization condition as

$$S_0(q) = \pm \int p \, dq. \tag{2.46}$$

The amplitude A diverges at the classical turning points at $p = 0$ where $S' = 0$. We introduce a linearization at the turning point $q = a$,

$$E - V(q) \approx F_0(x - a) \tag{2.47}$$

and solve the new Schrödinger equation

$$\frac{d^2\Psi}{dq^2} + \frac{2mF_0x}{\hbar^2}\Psi = 0. \tag{2.48}$$

Comparison of the wave functions with the Airy solutions leads to the following conditions for the wave function between the turning points $b < x < a$:

$$\Psi(q) \propto \cos\left(\frac{1}{\hbar}\int_q^a p\,dq - \frac{\pi}{4}\right) \overset{!}{\propto} \cos\left(\frac{1}{\hbar}\int_b^a p\,dq - \frac{\pi}{4}\right) \tag{2.49}$$

which leads to the WKB quantization condition

$$\int_b^a p\,dq = \pi\hbar\left(n + \frac{1}{2}\right), \quad n \in \mathbb{N}_0. \tag{2.50}$$

2.3.3 Torus quantization

For systems with two or more degrees of freedom, the quantization condition can be generalized to higher dimensions. We start with the Hamilton–Jacobi equation

$$H(\boldsymbol{q}, \nabla_{\mathbf{q}}S) - E = 0, \quad \boldsymbol{p} = \nabla_{\mathbf{q}}S. \tag{2.51}$$

The solution $S(\boldsymbol{q})$ is evaluated between the singularities

$$\det\left|\frac{\partial p_j}{\partial q_k}\right| \to \infty. \tag{2.52}$$

Analogously, we define

$$\bar{S}(\boldsymbol{p}) = S(\boldsymbol{q}) - \boldsymbol{p}\,\boldsymbol{q} \tag{2.53}$$

to obtain the following Hamilton–Jacobi equation

$$H(-\nabla_{\mathbf{p}}\bar{S}, \boldsymbol{p}) - E = 0, \quad \boldsymbol{q} = -\nabla_{\mathbf{p}}\bar{S}. \tag{2.54}$$

Maslov index

We choose $\sigma_{\mathbf{q}}(\boldsymbol{q})$ to be integer and define

$$\sigma_{\mathbf{p}} = \sigma_{\mathbf{q}}(\boldsymbol{q}) - \operatorname{sgn}\left(\frac{\partial p_l}{\partial q_m}\right). \tag{2.55}$$

In action–angle variables we obtain

$$J_k = \frac{1}{2\pi}\oint_{C_k} \boldsymbol{p}\, d\boldsymbol{q}, \quad \alpha_k = \frac{1}{2}[\sigma_{\mathbf{q}}]_{C_k}, \tag{2.56}$$

where α_k is the Maslov index. For the q-branch, the wave function is defined as

$$\Psi(\boldsymbol{q}, R) = B(\boldsymbol{q}, R)\exp\left(i\left(\frac{S(\boldsymbol{q})}{\hbar} - \sigma_{\mathbf{q}}\frac{\pi}{4}\right)\right) \tag{2.57}$$

and in the p-branch as

$$\Psi(\boldsymbol{p}, R) = \bar{B}(\boldsymbol{p}, R)\exp\left(i\left(\frac{\bar{S}(\boldsymbol{p})}{\hbar} - \sigma_{\mathbf{p}}\frac{\pi}{4}\right)\right) \tag{2.58}$$

where B and $\bar{B}$ are the amplitudes in the respective branches. The wave function has to be periodic along each trajectory C_k,

$$\frac{1}{\hbar}\left[S(\boldsymbol{q})\right]_{C_k} - [\sigma_{\mathbf{q}}]_{C_k}\frac{\pi}{4} = 2\pi n_k, \quad n_k \in \mathbb{N}_0, \quad k = 1, \ldots, f. \tag{2.59}$$

This leads to the quantization condition

$$J_k = \frac{1}{2\pi}\left[S(\boldsymbol{q})\right]_{C_k} = \hbar\left(n_k + \frac{\alpha_k}{4}\right), \quad \alpha_k = \frac{[\sigma_{\mathbf{q}}]_{C_k}}{2}. \tag{2.60}$$

The energy on each torus is conserved and classically defined as

$$E(\boldsymbol{n}) = E\left(\hbar\left(\boldsymbol{n} + \frac{\boldsymbol{\alpha}}{4}\right)\right) \tag{2.61}$$

where $\boldsymbol{n}$ is the set of quantum numbers associated with the action variables.

2.3.4 Einstein–Brillouin–Keller quantization

The Einstein–Brillouin–Keller (EBK) quantization condition is a semiclassical quantization rule that is applicable to higher-dimensional integrable systems. We continue with the Hamiltonian (cf. equation (2.37)) in action–angle variables. For an f-dimensional system, the EBK quantization condition states that the action variables J_i must take discrete values

$$J_i = \hbar\left(n_k + \frac{\alpha_k}{4}\right), \quad n_k \in \mathbb{N}_0, \quad k = 1, \ldots, f \tag{2.62}$$

and the trajectories in phase space lie on tori.

Berry-Tabor formula

The density of states for EBK-quantized tori can be written as

$$d(E) = \sum_n \delta(E - E(n))\,. \tag{2.63}$$

By applying Poisson summation and semiclassical analysis, one arrives at the Berry-Tabor formula [3] for a system with two degrees of freedom, which reads

$$d(E) = \tilde{d}^{(2)}(E) + \sum_{M\neq 0} C_M \cos\left(\frac{S_M}{\hbar} - \frac{\pi}{2}\sigma_M - \frac{\pi}{4}\right). \tag{2.64}$$

Here, the oscillatory terms originate from periodic trajectories on resonant tori. Their contributions appear as cosine terms with actions S_M, while the coefficients C_M encode stability and amplitude information. The smooth part $\tilde{d}^{(2)}(E)$ corresponds to the Thomas-Fermi contribution. By Fourier transforming the density of states, one can identify peaks at the periods of classical periodic orbits, thus revealing the classical dynamics imprinted in the quantum spectrum. In the special case of scaling systems, the relation between classical periods and quantum oscillations becomes particularly transparent, since all actions scale uniformly with energy. By Fourier transforming the density of states, one can identify peaks at the periods of classical periodic orbits, thus revealing the classical dynamics imprinted in the quantum spectrum.

2.4 Classical Dynamics of Periodic Orbits

2.4.1 Energy and action of periodic orbits

We now turn to periodic orbits of the exciton, where the number of revolutions (by 2π) is counted by the winding numbers w_e, w_h, and w_ρ respectively. For periodic orbits the ratios of the winding numbers are rational. Our goal is to establish the relation between the energy and the classical action associated with these orbits.

Inside the quantum well the potential is constant, so the electron and hole move with constant velocities $|v_\mathrm{e}|$ and $|v_\mathrm{h}|$, undergoing elastic reflections at the boundaries. For convenience, we work in scaled units and set the well width to $L = 1$.

The corresponding primitive periods of the electron and hole motion are

$$T_{\mathrm{e,h}} = \frac{2w_{\mathrm{e,h}}}{|v_{\mathrm{e,h}}|}. \tag{2.65}$$

The two-dimensional Coulomb problem is analogous to the Kepler problem and yields a radial period

$$T_\rho = 2\pi w_\rho \left(-2E_{\mathrm{kin},\rho}\right)^{-\frac{3}{2}} . \tag{2.66}$$

For periodic orbits, all three periods must coincide,

$$T_\mathrm{e} = T_\mathrm{h} = T_\rho . \tag{2.67}$$

The equality $T_\mathrm{e} = T_\mathrm{h}$ implies a relation between the electron and hole velocities,

$$\frac{|v_\mathrm{h}|}{|v_\mathrm{e}|} = \frac{w_\mathrm{h}}{w_\mathrm{e}} . \tag{2.68}$$

Using the kinetic energy definition

$$|v_\mathrm{e}|^2 = \frac{2E_\mathrm{kin,e}}{m_\mathrm{e}} , \tag{2.69}$$

the hole's kinetic energy can be expressed in terms of the electron's as

$$E_\mathrm{kin,h} = \frac{m_\mathrm{h}}{2}|v_\mathrm{h}|^2 = \frac{m_\mathrm{h}}{m_\mathrm{e}}\left(\frac{w_\mathrm{h}}{w_\mathrm{e}}\right)^2 E_\mathrm{kin,e} . \tag{2.70}$$

Finally, using $T_\mathrm{e} = T_\rho$ we obtain for the radial kinetic energy

$$E_{\mathrm{kin},\rho} = -\left(\frac{w_\rho}{w_\mathrm{e}}\right)^{2/3}\left(\frac{\pi^2 E_\mathrm{kin,e}}{4m_\mathrm{e}}\right)^{\frac{1}{3}} . \tag{2.71}$$

By combining (Eqs. (2.70), (2.71)), we obtain the total scaled energy of the exciton,

$$\tilde{E}_\mathrm{total} = LE_\mathrm{total} = \tilde{E}_\mathrm{kin,e} + \tilde{E}_\mathrm{kin,h} + \tilde{E}_{\mathrm{kin},\rho} . \tag{2.72}$$

Expressed in terms of $\tilde{E}_\mathrm{kin,e}$ this becomes

$$\tilde{E}_\mathrm{total} = \tilde{E}_\mathrm{kin,e}\left(1 + \frac{m_\mathrm{h}}{m_\mathrm{e}}\left(\frac{w_\mathrm{h}}{w_\mathrm{e}}\right)^2\right) - \left(\frac{w_\rho}{w_\mathrm{e}}\right)^{\frac{2}{3}}\left(\frac{\pi^2 \tilde{E}_\mathrm{kin,e}}{4m_\mathrm{e}}\right)^{\frac{1}{3}} . \tag{2.73}$$

For a given scaled energy $\tilde{E}_\mathrm{total}$ this relation leads to a cubic equation in $\tilde{E}_\mathrm{kin,e}$,

$$\begin{aligned}
&\tilde{E}^3_\mathrm{total} + \tilde{E}_\mathrm{kin,e}\left[\left(\frac{w_\rho \pi}{2w_\mathrm{e}\sqrt{m_\mathrm{e}}}\right)^2 - 3\tilde{E}^2_\mathrm{total}\left(1 + \frac{m_\mathrm{h}}{m_\mathrm{e}}\left(\frac{w_\mathrm{h}}{w_\mathrm{e}}\right)^2\right)\right] \\
&\quad + 3\tilde{E}^2_\mathrm{kin,e}\tilde{E}_\mathrm{total}\left(1 + \frac{m_\mathrm{h}}{m_\mathrm{e}}\left(\frac{w_\mathrm{h}}{w_\mathrm{e}}\right)^2\right)^2 \\
&\quad - \tilde{E}^3_\mathrm{kin,e}\left(1 + \frac{m_\mathrm{h}}{m_\mathrm{e}}\left(\frac{w_\mathrm{h}}{w_\mathrm{e}}\right)^2\right)^3 = 0 .
\end{aligned} \tag{2.74}$$

Solving this polynomial yields the scaled electron kinetic energy $\tilde{E}_{\mathrm{kin,e}}$ and thereby also the corresponding values for $\tilde{E}_{\mathrm{kin,h}}$ and $\tilde{E}_{\rho}$. Given the cubic structure either three or one real solutions exist. Each solution with $\tilde{E}_{\mathrm{kin,e}} \geq 0$ corresponds to a family of periodic orbits.

We now turn to the scaled classical actions. The electron and hole contributions inside the quantum well are

$$\tilde{S}_{\mathrm{e}} = 2w_{\mathrm{e}}\sqrt{2m_{\mathrm{e}}\tilde{E}_{\mathrm{kin,e}}}, \quad \tilde{S}_{\mathrm{h}} = \left(\frac{w_{\mathrm{h}}^2}{w_{\mathrm{e}}}\right)\sqrt{8\frac{m_{\mathrm{h}}^2}{m_{\mathrm{e}}}\tilde{E}_{\mathrm{kin,e}}}. \tag{2.75}$$

The radial action is defined as

$$\tilde{S}_{\rho} = 2\pi w_{\rho}\left(-2\tilde{E}_{\mathrm{kin},\rho}\right)^{-\frac{1}{2}}. \tag{2.76}$$

Using the definition of the total scaled energy, this can be rewritten as

$$\begin{aligned}
\tilde{S}_{\rho} &= 2\pi w_{\rho}\left(-2\left(\tilde{E}_{\mathrm{total}} - \left(\tilde{E}_{\mathrm{kin,e}} + \tilde{E}_{\mathrm{kin,h}}\right)\right)\right)^{-\frac{1}{2}} \\
&= 2\pi w_{\rho}\left(-2\left(\tilde{E}_{\mathrm{total}} - \left(\tilde{E}_{\mathrm{kin,e}} + \frac{m_{\mathrm{h}}}{m_{\mathrm{e}}}\left(\frac{w_{\mathrm{h}}}{w_{\mathrm{e}}}\right)^2\tilde{E}_{\mathrm{kin,e}}\right)\right)\right)^{-\frac{1}{2}} \\
&= 2\pi w_{\rho}\left(-2\left[\tilde{E}_{\mathrm{total}} - \tilde{E}_{\mathrm{kin,e}}\left(1 + \frac{m_{\mathrm{h}}}{m_{\mathrm{e}}}\left(\frac{w_{\mathrm{h}}}{w_{\mathrm{e}}}\right)^2\right)\right]\right)^{-\frac{1}{2}}.
\end{aligned} \tag{2.77}$$

Finally, the total action is given by

$$\begin{aligned}
\tilde{S}_{\mathrm{total}} &= \tilde{S}_{\mathrm{e}} + \tilde{S}_{\mathrm{h}} + \tilde{S}_{\rho} \\
&= 2w_{\mathrm{e}}\sqrt{2m_{\mathrm{e}}\tilde{E}_{\mathrm{kin,e}}} + \left(\frac{w_{\mathrm{h}}^2}{w_{\mathrm{e}}}\right)\sqrt{8\frac{m_{\mathrm{h}}^2}{m_{\mathrm{e}}}\tilde{E}_{\mathrm{kin,e}}} \\
&+ 2\pi w_{\rho}\left(-2\left[\tilde{E}_{\mathrm{total}} - \tilde{E}_{\mathrm{kin,e}}\left(1 + \frac{m_{\mathrm{h}}}{m_{\mathrm{e}}}\left(\frac{w_{\mathrm{h}}}{w_{\mathrm{e}}}\right)^2\right)\right]\right)^{-\frac{1}{2}}.
\end{aligned} \tag{2.78}$$

2.4.2 Visualization of periodic orbits

Movement in the radial direction

In order to investigate the time-dependence of the periodic orbits, we start with the equations of motion. The classical Hamiltonian for the exciton in exciton Hartree units is given by

$$E = \frac{p_{z,\mathrm{h}}^2}{2m_\mathrm{h}} + \frac{p_{z,\mathrm{e}}^2}{2m_\mathrm{e}} + \frac{\dot{\rho}^2}{2} - \frac{1}{\rho}. \tag{2.79}$$

Here, the first two terms correspond to the kinetic energies of the electron and hole in the quantum well, while the last two terms describe the radial motion and the Coulomb interaction.

For later convenience we introduce the effective radial energy by subtracting the electron and hole contributions from the total energy,

$$E_\rho \equiv E - E_{\mathrm{kin,e}} - E_{\mathrm{kin,h}} = \frac{\dot{\rho}^2}{2} - \frac{1}{\rho}. \tag{2.80}$$

Rearranging gives the radial equation of motion,

$$\dot{\rho} = \pm\sqrt{2\left(E_\rho + \frac{1}{\rho}\right)}, \tag{2.81}$$

which can be integrated in the form

$$\pm\frac{d\rho}{\sqrt{2\left(E_\rho + \frac{1}{\rho}\right)}} = dt. \tag{2.82}$$

By substituting $\tilde{\rho} = -\rho E_\rho$ we obtain

$$\pm\frac{1}{\sqrt{2}E_\rho}\frac{1}{\sqrt{-E_\rho}}\frac{d\tilde{\rho}}{\sqrt{\frac{1}{\tilde{\rho}} - 1}} = dt. \tag{2.83}$$

The solution of the integral leads to

$$\mp\frac{1}{\sqrt{2}E_\rho}\frac{1}{\sqrt{-E_\rho}}\left(E_\rho\rho\sqrt{-\frac{1}{E_\rho\rho} - 1} - \arctan\left(\sqrt{-\frac{1}{E_\rho\rho} - 1}\right)\right) + c_\mp = t \tag{2.84}$$

which describes the time evolution of the radial coordinate ρ in terms of the effective radial energy E_ρ and an integration constant $c_\pm$. We can later use this result to construct the full trajectories of the exciton with respect to the initial conditions.

Movement in z-direction

The exciton is confined in the z-direction by the quantum well potential. Inside the well, the velocities v_e and v_h of the electron and hole are constant. Upon reaching the

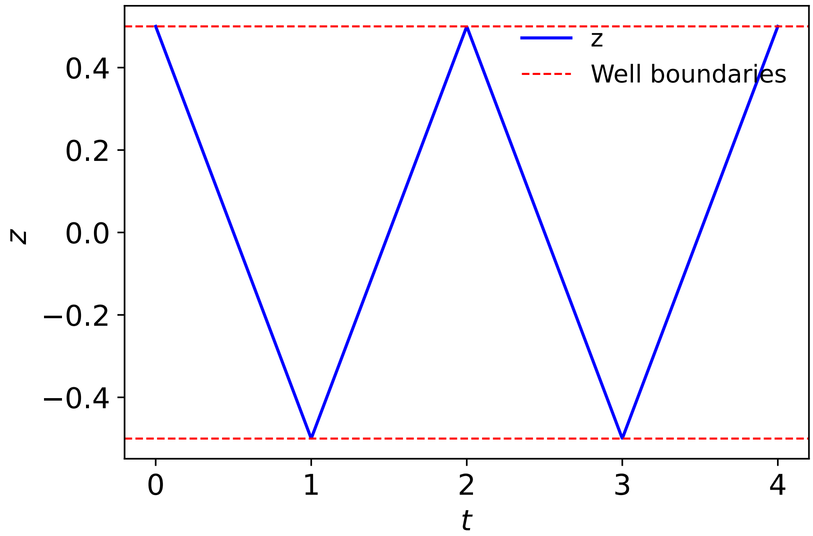

Figure 2.1: Classical motion of the exciton in the z-direction. The trajectory follows a triangular function, reflecting constant velocity between the well boundaries at $z = \pm\frac{1}{2}$ and elastic reflections at the edges.

boundaries of the well, they undergo elastic reflections. We denote the period for one cycle in the z-direction for the exciton with velocity $v_{\mathrm{e,h}}$ as

$$p_{\mathrm{e,h}} = \frac{2}{|v_{\mathrm{e,h}}|}. \tag{2.85}$$

The trajectories in the z-direction can be expressed as

$$z_{\mathrm{e,h}}(t, v) = \left| t \bmod p_{\mathrm{e,h}} - \frac{p_{\mathrm{e,h}}}{2} \right| \cdot \frac{2}{p_{\mathrm{e,h}}} - \frac{1}{2}. \tag{2.86}$$

As can be seen in fig. 2.1, this corresponds to a triangular trajectory where the exciton moves at constant velocity between the well boundaries at $z = \pm\frac{1}{2}$ and undergoes elastic reflections at the edges.

3 Results and Discussion

3.1 Exciton Energy Spectra in the Quantum Well

The first step in our analysis is to compute the exciton energies inside the quantum well as a function of the well width L. According to equation (2.25), the total scaled energy consists of the quantized contributions from the electron and hole motion in the z-direction, together with the two-dimensional Coulomb interaction,

$$E = \frac{\pi^2 \mu}{2(L/a_0)^2} \left(\frac{N_e^2}{m_e} + \frac{N_h^2}{m_h} \right) - \frac{1}{2n^2}. \tag{3.1}$$

The first term scales with $1/L^2$ and therefore dominates for small quantum well widths. The second term accounts for the Coulomb interaction, which gives a constant negative shift to the energy levels particularly for large quantum well widths. In fig. 3.1, we show the energy spectra for the exciton energy levels as a function of the quantum well width L for different combinations of (N_e, N_h, n). As expected the $1/L^2$ term causes the exciton energies to increase for smaller well widths, while for larger widths the energies approach the Coulomb limit. In the plot we see three different branches which correspond to the quantum number $n = 1, 2, 3, 4$ of the hydrogenic energy levels. The offset is created by the Coulomb term. For each branch the curves with the highest energy with quantum number triplets $(N_e, N_h, n) = (2, 2, 1), (2, 2, 2), (2, 2, 3), (2, 2, 4)$ are shown in colors blue, orange, green and red respectively. The Coulomb limit $-1/(2n^2)$ is indicated by the horizontal dashed lines.

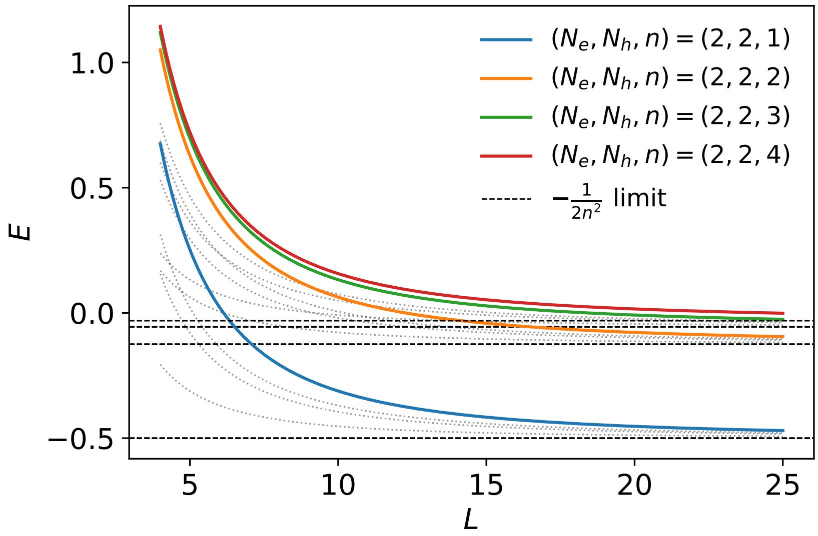

Figure 3.1: Exciton energy E as a function of the quantum-well width L for selected quantum numbers $(N_e, N_h, n) = (2, 2, 1), (2, 2, 2), (2, 2, 3), (2, 2, 4)$ in colors blue, orange, green and red respectively. For narrow wells the confinement contribution $\propto 1/L^2$ dominates and raises the energies, while for large L all branches approach the two-dimensional hydrogenic Coulomb limit $-1/(2n^2)$ (horizontal dashed). The gray dashed curves represent the remaining quantum number triplets.

3.2 Periodic Orbit Condition and Cubic Relation

Classical periodic orbits satisfy the commensurability condition

$$T_\mathrm{e} = T_\mathrm{h} = T_\rho, \tag{3.2}$$

which leads to a cubic equation (cf. equation (2.74)) for the scaled electron kinetic energy $x \equiv \tilde{E}_{\mathrm{kin},e}$ at fixed total scaled energy $\tilde{E}_\mathrm{total}$ and fixed winding numbers $(w_\mathrm{e}, w_\mathrm{h}, w_\rho)$. Introducing the abbreviations

$$r \;\equiv\; 1 + \frac{m_\mathrm{h}}{m_\mathrm{e}}\left(\frac{w_\mathrm{h}}{w_\mathrm{e}}\right)^2, \qquad C \;\equiv\; \left(\frac{w_\rho \pi}{2 w_\mathrm{e}\sqrt{m_\mathrm{e}}}\right)^2, \tag{3.3}$$

the cubic equation can be written as

$$\tilde{E}^3_\mathrm{total} + x\left(C - 3\tilde{E}^2_\mathrm{total} r\right) + 3x^2 \tilde{E}_\mathrm{total} r^2 - x^3 r^3 = 0 \tag{3.4}$$

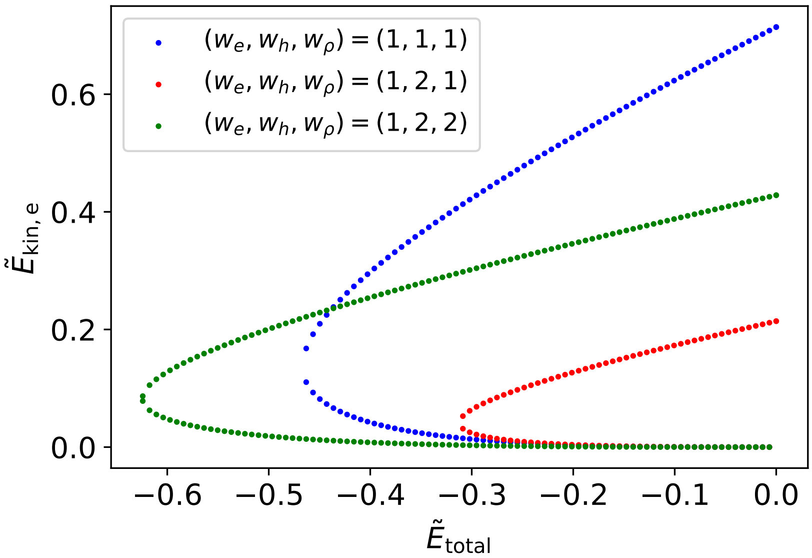

Figure 3.2: Physically relevant roots for the cubic equation (3.4) for three different combinations of winding numbers $(w_\mathrm{e}, w_\mathrm{h}, w_\rho) = (1,1,1), (1,2,1), (1,2,2)$ in colors blue, red, and green, respectively. The cubic polynomial gives two real solutions for each $\tilde{E}_\mathrm{total}$.

For a given integer triplet $(w_\mathrm{e}, w_\mathrm{h}, w_\rho)$, we sweep $\tilde{E}_\mathrm{total}$ and solve (cf. equation (3.4)) numerically using the NumPy function polyroots [4]. Each real root $x(\tilde{E}_\mathrm{total})$ that satisfies the criteria

$$x \;=\; \tilde{E}_{\mathrm{kin},e} \;\geq 0, \qquad \tilde{E}_\rho \;\equiv\; \tilde{E}_\mathrm{total} - \tilde{E}_{\mathrm{kin},e} - \tilde{E}_{\mathrm{kin},h} \;=\; \tilde{E}_\mathrm{total} - rx \;<\; 0, \tag{3.5}$$

corresponds to a family of periodic orbits. The set of admissible solutions can form up to three continuous branches $x(\tilde{E}_\mathrm{total})$.

Fig. 3.2 shows the results for three different sets of winding numbers where we can see the splitting of the solutions into two branches.

3.2.1 Classical trajectories of periodic orbits

Trajectory in z-direction

As established above, in the classical model the exciton reflects elastically at both borders of the quantum well. The motion in the z-direction is uniform upon reflection while each winding number determines the number of reflections at the boundaries for the electron and hole respectively. The trajectories $z_\mathrm{e}(z_\mathrm{h})$, $z_\mathrm{e}(\rho)$, $z_\mathrm{h}(\rho)$ for winding numbers $(w_\mathrm{e}, w_\mathrm{h}, w_\rho) = (1,1,1), (1,2,1), (1,3,1), (2,3,4), (3,5,4)$ can be seen in figs.

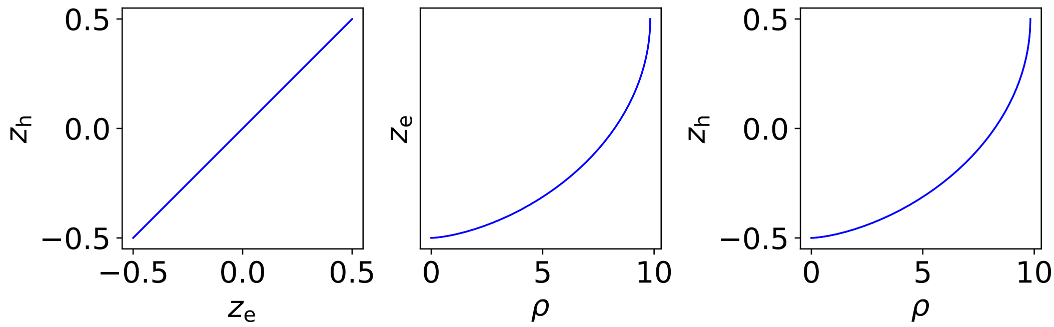

Figure 3.3: Classical trajectories $z_e(z_h)$, $z_e(\rho)$, $z_h(\rho)$ of the exciton in the quantum well. The electron and hole move uniformly inside the quantum well, while the winding numbers w_e, w_h and w_ρ determine the number of reflections at the boundaries. The figure consists of plots for winding number pairs $(w_e, w_h, w_\rho) = (1, 1, 1)$.

(3.3, 3.4, 3.5, 3.6, 3.7). By changing the combinations of the winding numbers to $(w_e, w_h, w_\rho) = (2, 3, 4), (3, 5, 4), (2, 5, 5)$ we can see that the number of reflections at the boundaries in z changes accordingly, which creates figures with multiple corners as can be seen in figs. (3.5, 3.6, 3.7). The number of corners tends to increase as the ratio of the winding numbers w_e/w_h increases.

Trajectory in ρ-direction

In order to compute the trajectory in the ρ-direction we solve the equations of motion for the radial coordinate ρ (cf. equation (2.81)). We use the implicit definition of ρ (cf. equation (2.84)) in order to calculate the time steps t. With each time step t we compute the corresponding $z_{e,h}$-values. Increasing the ratio of the winding numbers w_ρ/w_h leads to more complex patterns in the (z_h, ρ) plane. The trajectories follow similar paths to the trajectories in the z-direction (cf. figure 3.5) but are modified by the radial motion of the exciton.

3.2.2 Classical actions of periodic orbits

By using the cubic equation (cf. equation (3.4)) we can compute the physically relevant kinetic energies $E_{\text{kin,e}}$ and sweep the scaled total energy $\tilde{E}_{\text{total}}$ in order to extract the total action of the periodic orbits (cf. equation (2.78)) for different combinations of winding numbers (w_e, w_h, w_ρ). We can see $\tilde{E}_{\text{total}}(\tilde{S}_{\text{total}})$ in fig. 3.8. Each color corresponds to the radial winding number w_ρ. The curves split into groups based on their radial winding number ρ where the curves corresponding to higher w_ρ are shifted down. Because of

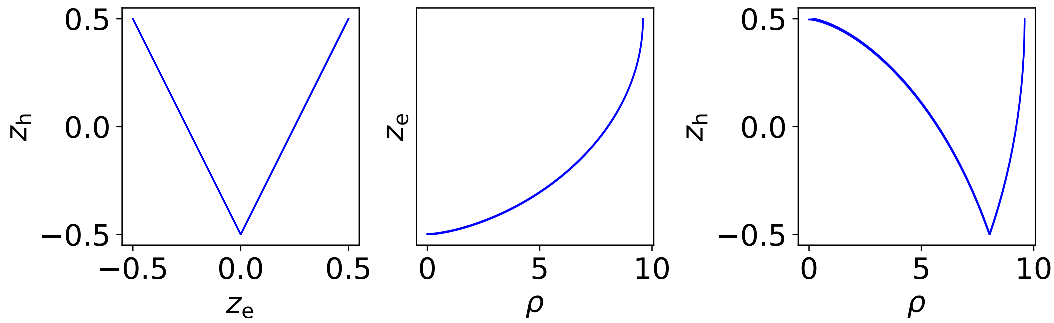

Figure 3.4: Classical trajectories $z_e(z_h)$, $z_e(\rho)$, $z_h(\rho)$ of the exciton in the quantum well. The electron and hole move uniformly inside the quantum well, while the winding numbers w_e, w_h and w_ρ determine the number of reflections at the boundaries. The figure consists of plots for winding number pairs $(w_e, w_h, w_\rho) = (1, 2, 1)$.

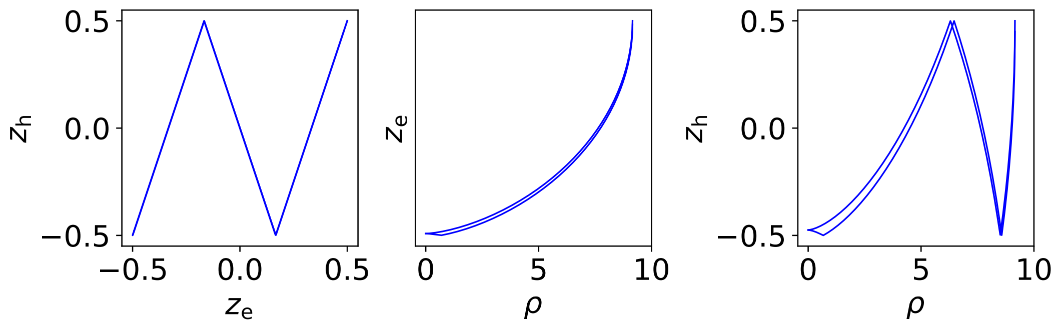

Figure 3.5: Classical trajectories $z_e(z_h)$, $z_e(\rho)$, $z_h(\rho)$ of the exciton in the quantum well for higher ratios of the winding numbers, i.e., $(w_e, w_h, w_\rho) = (1, 3, 1)$. The number of corners increases with the ratio w_e/w_h.

the multiple solutions for the kinetic energy of the Electron $\tilde{E}_{\mathrm{kin,e}}$ (cf. figure 3.2), the curves split into two branches. Furthermore, each branch corresponds to all possible ratios w_e/w_h, where w_e, $w_h \leq 4$.

3.3 Semiclassical Density of States and Spectral Properties

After calculating the classical trajectories of periodic orbits and their corresponding scaled actions, we can now use this information to compare the classical scaled action and its scaled energy to the Fourier transform of the semiclassical density of states in

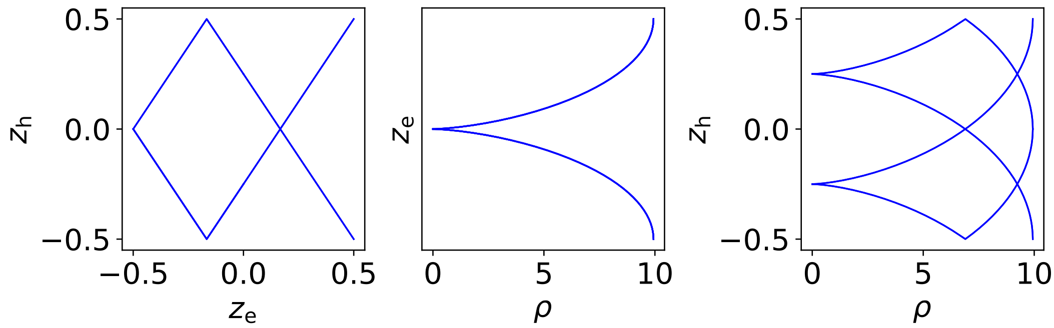

Figure 3.6: Classical radial trajectories of the exciton in the $z_e(z_h)$, $z_e(\rho)$, $z_h(\rho)$ plane for winding numbers $(w_e, w_h, w_\rho) = (2, 3, 4)$. The trajectories illustrate the periodic motion confined by the quantum well boundaries.

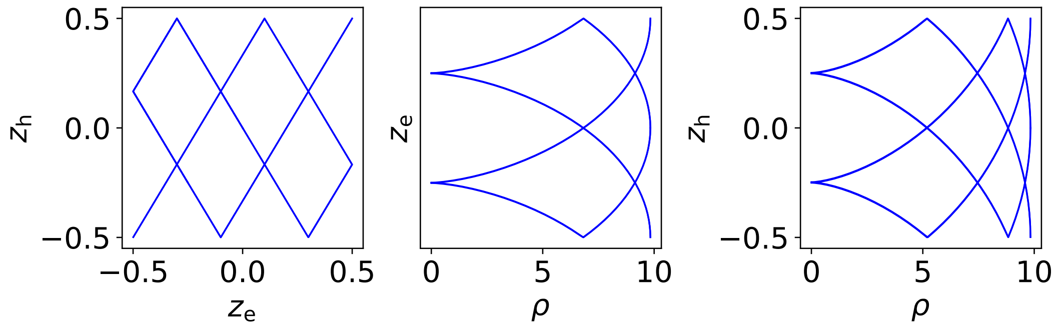

Figure 3.7: Exciton radial trajectories in the $z_e(z_h)$, $z_e(\rho)$, $z_h(\rho)$ plane for winding number triplet $(w_e, w_h, w_\rho) = (3, 5, 4)$. Increasing the winding ratio modifies the periodic structure of the orbit and demonstrates the transition toward more complex trajectories within the well.

order to confirm the location of peaks in the spectrum with the scaled actions and scaled energies of the periodic orbits, cf. the Berry-Tabor-formula (2.64).

3.3.1 Density of states for periodic orbits

We start with the scaled total energy

$$\tilde{E}_{\text{total}} = LE = \frac{\pi^2 \mu a_0^2}{2L} \left(\frac{N_e^2}{m_e} + \frac{N_h^2}{m_h} \right) - \frac{L}{2n^2} \tag{3.6}$$

and multiply L in order to obtain a quadratic equation of form

$$\frac{L^2}{2n^2} + L\tilde{E}_{\text{total}} - \frac{\pi^2 \mu a_0^2}{2} \left(\frac{N_e^2}{m_e} + \frac{N_h^2}{m_h} \right) = 0. \tag{3.7}$$

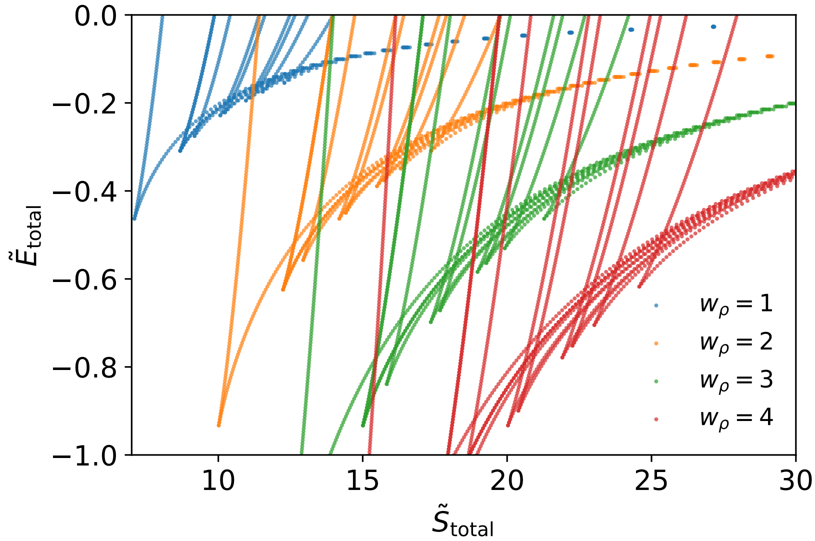

Figure 3.8: Scaled total energy over total scaled action of the periodic orbits. The curves build groups with respect to their radial winding number $w_\rho = 1, 2, 3, 4$ marked in blue, orange, green and red.

The physically relevant positive root $L_{N_e,N_h,n}$ of the quadratic equation is

$$L_{N_e,N_h,n}(\tilde{E}_{\text{total}}) = n^2 \left(-\tilde{E} + \sqrt{\tilde{E}^2 + \frac{\pi^2 \mu a_0^2}{n^2} \left(\frac{N_{\text{e}}^2}{m_{\text{e}}} + \frac{N_{\text{h}}^2}{m_{\text{h}}} \right)} \right) . \tag{3.8}$$

In section 2.3.4 we defined the density of states (cf. equation (2.63)) as a function of the energy. In our case the density of states is a function of $\sqrt{L}$

$$\rho\left(\sqrt{L}\right) = \sum_{N_e,N_h,n} \delta\left(\sqrt{L} - \sqrt{L_{N_e,N_h,n}}\right) . \tag{3.9}$$

By using our solution for $L_{N_e,N_h,n}$ (cf. equation (3.8)) we arrive at

$$\rho(\sqrt{L}) = \sum_{N_e,N_h,n} \delta\left(\sqrt{L} - \sqrt{n}\sqrt{\left[n^2\tilde{E}^2 + \pi^2\mu a_0^2\left(\frac{N_e^2}{m_e} + \frac{N_h^2}{m_h}\right)\right]^{1/2} - \tilde{E}}\right) . \tag{3.10}$$

3.3.2 Spectral analysis and comparison to classical periodic orbits

Using equation (3.8), we can obtain the allowed values of the quantum well width L for a given scaled energy $\tilde{E}_{\text{total}}$. Plotting $\tilde{E}_{\text{total}}$ as a function of $\sqrt{L}$ provides a convenient way to visualize the density of states. Regions where many solutions accumulate correspond to a high density of states, while sparsely populated regions indicate gaps.

Figure 3.9 shows the resulting spectrum for all combinations of quantum numbers $N_e, N_h, n < 15$. A high density of states can be observed for $5 < \sqrt{L} < 12.5$ in the energy interval $-1.5 < \tilde{E}_{\text{total}} < 0.5$ in exciton Hartree units. In contrast, outside this interval the solutions become more dilute, on the right hand side due to the cut-off of quantum numbers in equation (3.8).

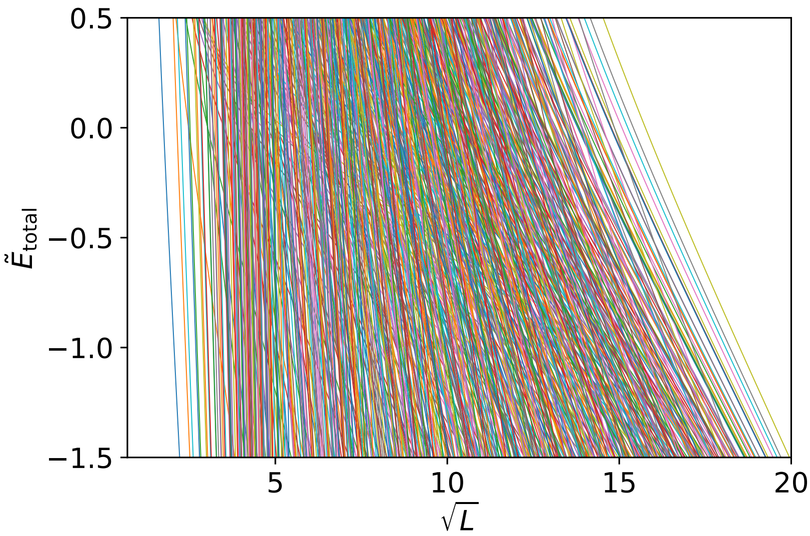

Figure 3.9: Scaled exciton energy $\tilde{E}_{\text{total}}$ as a function of the scaled quantum well width $\sqrt{L}$. Regions of high density of solutions correspond to an enhanced density of states.

Furthermore, we can use the Fourier transform in order to analyze the spectral properties of the density of states. By applying the transformation on the density of states we arrive at

$$f(\tilde{S}) = \int_{\sqrt{L_1}}^{\sqrt{L_2}} \rho(\sqrt{L}) \exp\left(i\tilde{S}\sqrt{L}\right) d\sqrt{L} = \sum_{N_e,N_h,n} \exp\left(i\tilde{S}\sqrt{L_{N_e,N_h,n}}\right). \tag{3.11}$$

The Fourier transform of the density of states for different scaled total energies $\tilde{E}_{\text{total}} = (-0.1, -0.3, -0.7)$ with quantum number combinations $N_{\text{e}}, N_{\text{h}}, n < 11Aa$ is shown in fig. 3.10 in combination with the scaled total energy as a function of the scaled total action for winding number triplets $w_{\text{e}}, w_{\text{h}}, w_\rho \leq 5$. We can see peaks in the Fourier spectrum at intersections of the horizontal lines with the curves of $\tilde{E}_{\text{total}}(\tilde{S}_{\text{total}})$. These peaks correspond to the actions of classical periodic orbits. Additional peaks can be observed because the Fourier transform resolves orbits with higher winding numbers $w_{\text{e}}, w_{\text{h}}, w_\rho > 5$.

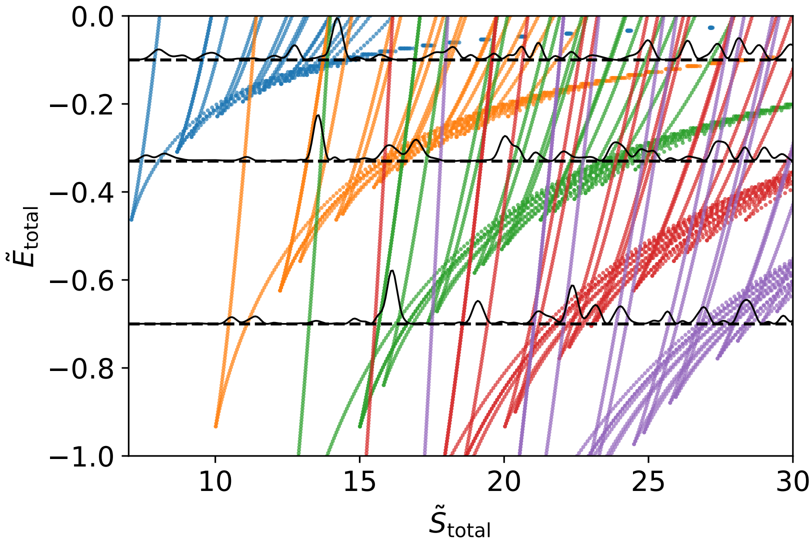

Figure 3.10: Scaled total energy $\tilde{E}_{\mathrm{total}}$ as a function of the scaled total action $\tilde{S}_{\mathrm{total}}$. The Fourier transform of the density of states (cf. equation (3.11)) is included for certain total scaled energies $\tilde{E}_{\mathrm{total}} = (-0.1, -0.3, -0.7)$ where peaks in the spectrum correspond to the actions of classical periodic orbits.

The scaled energy as a function of the scaled action can be seen in fig. 3.10, where we highlighted the occurrences of peaks of the Fourier transform. We can see in the Berry-Tabor formula (cf. equation (2.64)) that the density of states oscillates with frequencies given by the actions of periodic orbits. The peaks in the Fourier transform therefore correspond to the actions of classical periodic orbits. We see in fig. 3.10 that the peaks align with the predicted actions from semiclassical periodic orbit theory.

4 Summary

4.1 Conclusions and Outlook

In this thesis we have computed and analyzed the scaled spectra of excitons in a quantum well with two-dimensional Coulomb interaction by combining semiclassical methods, classical periodic orbit theory, and numerical calculations. Starting from the Hamiltonian formulation we derived the periodic orbit condition and established a cubic relation between the scaled total energy and the kinetic energy contributions of electron and hole motion. This allowed us to identify families of classical trajectories and to compute their associated classical actions.

The exciton energy spectra obtained from the quantum well model exhibit the expected confinement dependence, interpolating between the $1/L^2$ scaling for narrow wells and the Coulombic limit for large well widths. By Fourier transforming the semiclassical density of states we revealed distinct peaks that correspond to the actions of classical periodic orbits. The comparison of the spectral analysis with the Berry–Tabor formula confirmed that these peaks are direct manifestations of the underlying classical dynamics. This demonstrates how periodic orbits leave measurable fingerprints in the exciton spectrum.

While the model captures the essential features of the semiclassical behavior, it also relies on several simplifying assumptions, most notably the reduction of the Coulomb potential to a two-dimensional form and the neglect of center-of-mass motion. These approximations enable analytic progress but limit the quantitative accuracy compared to real cuprous oxide quantum wells.

Bibliography

[1] Pavel A. Belov, Florian Morawetz, Sjard Ole Krüger, Niklas Scheuler, Patric Rommel, Jörg Main, Harald Giessen, and Stefan Scheel. "Energy states of Rydberg excitons in finite crystals: From weak to strong confinement". In: *Phys. Rev. B* 109 (2024), p. 235404. DOI: 10.1103/PhysRevB.109.235404.

[2] Niklas Scheuler, Patric Rommel, Jörg Main, and Pavel A. Belov. "Resonance energies and linewidths of Rydberg excitons in cuprous oxide quantum wells". In: *Phys. Rev. B* 109 (2024), p. 165440. DOI: 10.1103/PhysRevB.109.165440.

[3] Jörg Main. *Nichtlineare Dynamik: An Introduction.* Lecture notes, University of Stuttgart. 2015.

[4] NumPy Developers. *NumPy Reference Manual.* Version 2.3; accessed 19 Sep 2025. 2025. URL: https://numpy.org/doc/stable/reference/.

[5] Wikipedia contributors. *Langer correction — Wikipedia, The Free Encyclopedia.* [Online; accessed 19-August-2025]. 2024. URL: https://en.wikipedia.org/wiki/Langer_correction.

[6] Angelos Aslanidis, Jörg Main, Patric Rommel, Stefan Scheel, and Pavel A. Belov. "Bound states in the continuum in cuprous oxide quantum wells". In: *Phys. Rev. B* 111 (2025), p. L121103. DOI: 10.1103/PhysRevB.111.L121103.

[7] Sandro Wimberger. *Nonlinear Dynamics and Quantum Chaos: An Introduction.* 2nd ed. Springer, 2022. ISBN: 978-3-031-01248-8. DOI: 10.1007/978-3-031-01249-5.

[8] Charles Kittel. *Introduction to Solid State Physics.* Jon Wiley & Sons, 2005. ISBN: 0-471-41526-X.

[9] Matthias Brack and Rajat K. Bhaduri. *Semiclassical Physics.* CRC Press, 2003. ISBN: 978-0-8133-4084-5.

Acknowledgements

First of all, I would like to thank Prof. Jörg Main, Dr. Patric Rommel, and Dr. Jan Ertl. Their guidance and support made this thesis possible, and I really appreciate how much I learned from them about both physics and the everyday life of research. I am also grateful to Niklas Scheuler. Last but not least, I would like to thank Mrs. Bund for keeping everything running smoothly and for always being attentive to everyone at the institute.

Erklärung

Ich versichere,

- dass ich diese Bachelorarbeit selbstständig verfasst habe,
- dass ich keine anderen als die angegebenen Quellen benutzt und alle wörtlich oder sinngemäß aus anderen Werken übernommenen Aussagen als solche gekennzeichnet habe,
- dass die eingereichte Arbeit weder vollständig noch in wesentlichen Teilen Gegenstand eines anderen Prüfungsverfahrens gewesen ist,
- und dass das elektronische Exemplar mit den anderen Exemplaren übereinstimmt.

Stockholm, den 20.09.2024 *David Mayer*